Korean J. Chem. Eng., 34(10), 2597-2609 (2017)
DOI: 10.1007/s11814-017-0167-1

pISSN: 0256-1115
eISSN: 1975-7220

A study on the direct catalytic steam gasification of coal for the bench-scale system

Tae-Jin Kang*, HyeJung Park, Hueon Namkung***, Li-Hua Xu**, Jung-Hyun Park*, Iljeong Heo*, Tae-Sun Chang*, Beom Sik Kim****, and Hyung-Taek Kim**,†**

*Carbon Resources Institute, Greenhouse Gas Resources Research Group, Korea Research Institute of Chemical Technology, 141 Gajeongro, Yuseong, Daejeon 34114, Korea
**Department of Energy Systems Research, Graduate School, Ajou University, Wonchon-dong, Yeongtong-gu, Suwon 16499, Korea
***Institute of Clean Coal Technology, East China University of Sci. & Tech., 130 Meilong Rd, Xuhui, Shanghai, 200237, China
****Carbon Resources Institute, CO2 Energy Vector Research Group, Korea Research Institute of Chemical Technology, 141 Gajeongro, Yuseong, Daejeon 34114, Korea
(*Received 6 February 2017 • accepted 20 June 2017*)

Abstract−Various techniques have been developed to increase the efficiency of coal gasification. The use of a catalyst in the catalytic-steam gasification process lowers the activation energy required for the coal gasification reaction. Catalytic-steam gasification uses steam rather than oxygen as the oxidant and can lead to an increased H_2/CO ratio. The purpose of this study was to evaluate the composition of syngas produced under various reaction conditions and the effects of these conditions on the catalyst performance in the gasification reaction. Simultaneous evaluation of the kinetic parameters was undertaken through a lab-scale experiment using Indonesian low rank coals and a bench-scale catalytic-steam gasifier design. The composition of the syngas and the reaction characteristics obtained in the lab- and bench-scale experiments employing the catalytic gasification reactor were compared. The optimal conditions for syngas production were empirically derived using lab-scale catalytic-steam gasification. Scale-up of a bench-scale catalytic-steam gasifier was based on the lab-scale results based on the similarities between the two systems. The results indicated that when the catalytic-steam gasification reaction was optimized by applying the K_2CO_3 catalyst to low rank coal, a higher hydrogen yield could be produced compared to the conventional gasification process, even at low temperature.

Keywords: Low Rank Coal, Fluidized-bed Reactor, Direct Catalytic-steam Gasification, K_2CO_3

INTRODUCTION

Currently, 80% of the energy consumed globally is derived from fossil fuels. Fossil fuel combustion is the most significant contributor to global warming. The need for an urgent response to the issue of climate change is emerging as a topical discussion in accordance with the Fifth Assessment Report of the Intergovernmental Panel on Climate Change (IPCC) [1]. Clean coal technology (CCT) is an important factor in achieving the goals set for climate change, and this factor requires an increase in the efficiency of coal-fired power plants, as well as Carbon Capture & Storage (CCS) [2].

Coal gasification technology is used to convert the carbon and hydrogen components of coal into syngas. The main components of syngas are gaseous carbon monoxide and hydrogen. Coal gasification is generally carried out at temperatures above 1,000 °C. Low rank coal can be gasified at a lower temperature, but the cold gas efficiency is not high in a fluidized bed. Although fluidized bed gasifiers are commonly operated at around 850-950 °C, the issue of bed agglomeration is a major limitation. Coal gasification at temperatures below 800 °C has been widely examined [3-13]. In other words, the development of coal gasification is hampered by several disadvantages, including high reaction temperatures, large energy consumption, difficult purification of the products, and stringent requirements for the process equipment. Coal gasification is also recognized to cause serious environmental pollution. To resolve some of these issues, a catalytic-steam coal gasification technique was previously developed to improve the reaction rate and conversion compared to those of conventional gasification techniques [14].

In catalytic-steam gasification, the gasification reaction is catalyzed even at relatively low temperatures and leads to changes in the composition of the syngas. Using a catalyst can significantly enhance the gasification rate at lower temperatures. Thus, catalytic-steam gasification has the important advantage of enhancing syngas production by decreasing the high pressure and temperature required for the gasification reaction [5-10,15-19]. However, catalytic-steam gasification has a problem such as economics and pollution. Catalytic-steam gasification should be recovered of catalyst which mainly influences the economic evaluation of this process. Another problem is soil/water pollution, which is caused by water-soluble alkali metal compounds existing in ash that do not un-

†To whom correspondence should be addressed.
E-mail: htkim@ajou.ac.kr
‡5th International Conference on Gasification and Its Application.

Table 1. Results of proximate and ultimate analyses of Indonesian low rank coals

Item	Coal	Indonesian lignite	MSJ	Roto south
Proximate analysis wt% (As received basis)	Moisture	32.10	17.16	1.12
	Volatile matter	34.25	38.02	48.75
	Fixed carbon	30.36	41.44	47.95
	Ash	3.30	3.37	2.19
Ultimate analysis wt% (Dry ash free basis)	C	52.21/51.69*	61.72/59.66*	58.19/57.16*
	H	4.04/4.09*	4.96/4.60*	4.73/4.25*
	O	42.49/43.00*	31.50/34.12*	35.78/37.42*
	N	0.38/0.36*	0.87/0.80*	0.44/0.37*
	S	0.88/0.86*	0.95/0.82*	0.86/0.80*
HHV, kcal/kg (Dry Basis)		6,078	6,971	6,154

*K_2CO_3 impregnation coal data

dergo catalyst recovery treatment [20].

Exxon studied the recovery of catalyst as potassium. This is called a digestion process, which uses water washing and lime treatment [21]. Sheth et al. investigated the recovery of catalyst, which method is extraction schemes such as water extraction, H_2SO_4 extraction, and acetic acid extraction [22]. Also, the China ENN Energy group studied catalyst recovery technology. This process contains two stages as water washing and digestion washing stage [23].

When low rank coals are utilized, a high carbon conversion is expected even at low temperature because of the good reactivity of these coals. Moreover, fixed-bed or fluidized bed reactors are generally used to process low rank coal [24]. Fluidized bed gasifiers are utilized instead of an entrained gasifier because the former has a relatively short residence time, which ensures the appropriate residence time required for gasification. Furthermore, during the gasification reaction, the endothermic reaction, the exothermic methanation reaction, and the exothermic water gas shift that occur during the direct catalytic-steam gasification process require less energy than in the existing gasification process [25].

With the objective of determining the optimal reaction conditions and the parameters affecting the performance of the catalytic-steam gasification process for syngas production, along with the kinetic conditions, a lab-scale experiment was performed using Indonesian low rank coal. The catalytic activity in catalytic gasification is influenced by physical properties of the catalyst and the coal itself, as well as the reaction of the composition present in the ash. In the order of the periodic table, group 1 alkali metals present the greatest activities, and the activity of the catalyst declines in the order of group 2 alkaline earth metals and then transition metal-based compounds [26]. Also, many researchers have confirmed that K_2CO_3 has better catalytic activity than other catalysts [14,26-29]. The characteristics of the syngas produced by bench-scale catalytic-steam gasification were also determined. To investigate the utilization of low rank coal, three Indonesian low rank coals were subjected to catalytic-steam gasification and the reaction kinetics and the composition of generated syngas was analyzed. The reactions employing the lab- and bench-scale fluidized bed reactors were also compared. To determine the parameters for the design of a bench-scale fluidized catalytic gasification reactor, a lab-scale reactor was used to determine the residence time and kinetic data by taking into account the similarities of these reactors, such as the volume and L_h/D (Length/Diameter).

EXPERIMENT AND METHODS

1. Characteristics of Coal Sample

Indonesian low rank coal is a high grade low rank coal with high moisture content but low ash content. Table 1 shows the characterization data for Indonesian lignite, MSJ, and Roto South employed for the catalytic gasification reaction.

2. Selection of Catalyst

Catalysts are often used to produce specific syngas products by increasing the selectivity of the reaction. The metal components in coal, artificially added transition metal oxides, or alkali metal oxides are typically used as catalysts. Studies of the effects of these metals on the catalyzed and un-catalyzed reactions have been reported [26,30,31]. The catalyst lowers the activation energy of the reaction [32]. It is well known that the reactivity of coal and char is increased by alkaline materials. Thus, K_2CO_3 was selected as a catalyst herein based on its high reactivity in coal gasification.

3. Impregnation of Catalyst (K_2CO_3)

The characteristics of the gasification reaction may differ based on the method used for catalyst mixing. Therefore, the composition of the syngas produced using the impregnation method employing an alkali ion catalyst and coal was compared with that produced using the physically mixed catalyst mixture of coal and catalyst combined through physical stirring. Furthermore, the impregnation process was conducted by adding the alkali-based catalyst (K_2CO_3) to water to create an aqueous solution, and then placing the coal in this aqueous solution and stirring for 6 h at 80 °C. Finally, the coal was dried for 24 h at 80 °C. K_2CO_3 is known to have an excellent impact on the rate of coal gasification. Table 2 lists the characteristics of the low rank coal and impregnated coal for comparison.

Comparison of the raw coal and impregnated coal indicated that the components (Mg, Al, Si, Ca, and Fe) were equally reduced, whereas the K content increased. These results show that K_2CO_3 was impregnated into the coal at a loading of 10 wt%.

Table 2. Comparison of results for low rank coal and K_2CO_3 impregnated coal

	Indonesian lignite		MSJ		Roto south	
	Raw (%)	Imp.* (%)	Raw (%)	Imp.* (%)	Raw (%)	Imp.* (%)
Na	-	0.04	1.21	0.44	-	0.16
Mg	1.10	0.20	0.87	0.23	1.82	0.32
Al	0.35	0.06	1.58	0.37	3.09	0.51
Si	0.84	0.13	1.32	0.32	5.16	0.93
P	-	-	0.04	0.01	0.03	-
S	3.01	0.61	45.08	8.20	4.60	2.99
Cl	-	0.02	-	-	-	0.03
K	0.24	74.63	0.38	74.7	0.47	79.30
Ca	22.54	10.33	24.96	7.36	27.64	8.73
Ti	-	-	-	-	1.20	0.18
Mn	1.00	0.19	-	-	0.65	0.07
Fe	70.46	13.72	23.23	7.99	55.05	6.51
Zn	0.41	-	-	-	-	-
Sr	-	-	0.16	0.10	0.24	0.05
Sn	-	-	1.09	0.24	-	0.17

Imp.*: Impregnation

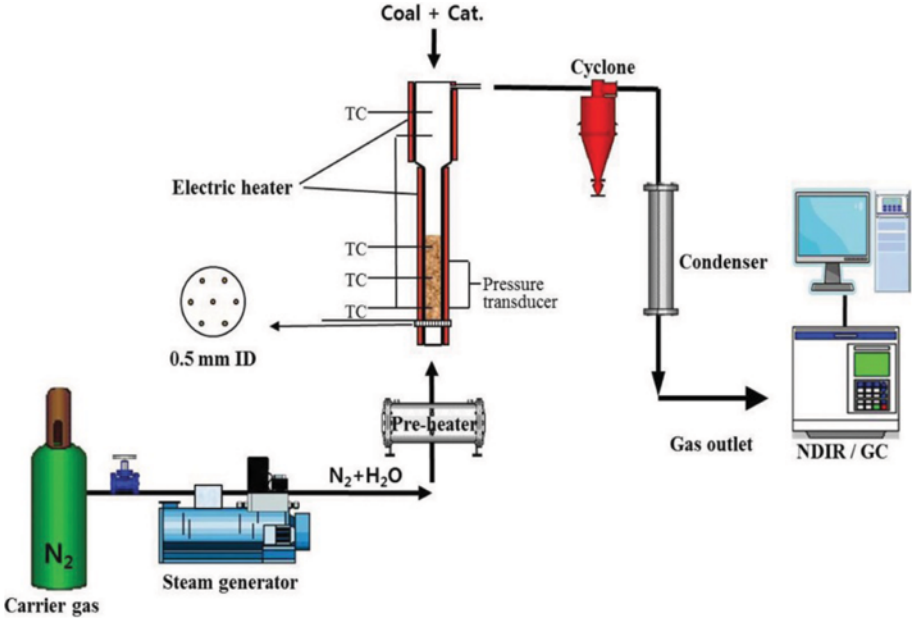

Fig. 1. Lab-scale direct catalytic-steam coal gasification system.

4. Experimental Apparatus and Procedure

The experimental process is summarized in Fig. 1. The lab-scale fluidized bed reactor was batch type, and the bench-scale reactor was continuous type; these consisted of components such as the N_2 carrier gas, steam generator, pre-heater, fluidized bed reactor, main heater, thimble filter, condenser and tar removal device, real-time gas analyzer, data logger, gas chromatograph (GC), and personal computer (PC).

The steam from the steam generator was injected into the reaction region, and the N_2 flow rate was set to 1.5 times U_{mf}. N_2 was used as the carrier gas because of bubbling and the limitation of carbon. However, the catalytic gasification involved using steam as the oxidant. Catalytic-steam gasification was conducted by simultaneously heating the electric furnace to raise the temperature to the desired reaction temperature and injecting the coal sample into the reactor when the desired reaction temperature was reached. A mixing chamber was installed on the pre-heater for mixing the steam and N_2.

The experimental parameters were as follows: the coal particle size was 0.85-1.18 mm; the temperature was varied as 600 °C, 700 °C, and 800 °C, and the catalyst (K_2CO_3) loading was set at 5 wt% and 10 wt% for the physical mixing injection method and 10 wt% for

the impregnation injection method. Catalytic-steam gasification has the characteristics as catalyst impregnation is more effective than physical mixing with the carbon [33]. Thus, this study carried out catalyst impregnation/physical mixing to evaluate the effect of the catalyst input method. The H_2O/C mole ratio was set to unity and the gas velocity was fixed at U_{mf}×1.5. The reaction temperature is one of the most important operating variables affecting the performance of the gasifier, since the main reaction in the gasification process is endothermic. Hence, the reaction temperature was considered as an experimental parameter in this study. Considering the deactivation of coal itself at 500 °C and the melting point of K_2CO_3 of 891 °C, the experimental temperature was set to below 800 °C to prevent decomposition and deactivation of the catalyst. Optimal gasification was achieved at a catalyst (K_2CO_3) loading of 10 wt%. At higher catalyst loading, a loss of reactivity was observed due to saturation of the system with the catalyst. Moreover, it has been reported that an excess of the mixed catalyst results in accumulation in the pores of coal, reducing the surface area of the porous carbon and limiting the coal gasification. Therefore, the amount of catalyst employed in the reaction was limited to 10 wt% [6,34-37].

5. Method for Scale Up of Lab-scale Fluidized Bed to Bench-scale

The parameters determined from catalytic-steam gasification using the lab-scale fluidized bed reactor were utilized as the design parameters for the bench-scale fluidized bed gasifier. Table 3 lists the design process steps for the bench-scale fluidized bed. In the design of the bench-scale catalytic-steam gasification system, 1 kW catalytic-steam gasification capacity (20 kg/day) was first selected. Second, the reaction time for the lab-scale fluidized bed was confirmed by introduction of different amounts of coal, as shown in Fig. 2. Fig. 2 shows that identical trends were obtained for the reaction rate when 10 g of coal was used, and the U_{mf} was double that amount. The resulting capacity of the lab-scale reactor was 4.3 kg/day with a 5 g reaction scale. MSJ coal was selected for the kinetic analysis because certain reactions of this coal are less dependent on temperature. Kang et al. reported about the dependence on temperature using Indonesian lignite, MSJ, Roto South coal [38]. The report mentioned that these samples showed higher pre-exponential factors, which implied that the influence of temperature on the pyrolysis of volatile matter was very low. Among these samples, MSJ showed the highest pre-exponential factors. Third, the volume of the bench-scale fluidized bed was calculated.

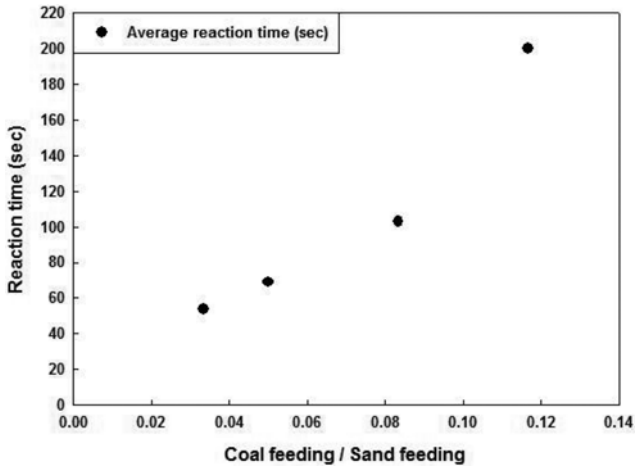

Fig. 2. Reaction time for lab-scale fluidized bed.

The capacity of the lab-scale fluidized bed catalytic-steam gasification reactor was approximately 4.3 kg/day. Therefore, a 4.6-fold scale-up was necessary in order to increase the scale to 20 kg/day. The L_h/D of the bed material (sand) of the lab-scale reactor was 3, which is approximately 60 g. Thus, approximately 280 g of bed material was needed to increase the capacity by 4.6-fold. The bulk density of the sand that was used was 1.3887 g/cm^3. Thus, the bench-scale fluidized bed required 400 g of bed material. Fourth, the diameter of the bench-scale fluidized bed was determined. The diameter of the reactor was determined using the sand bulk density and volume or weight, as listed in Table 4. The minimum fluidization velocity was 19.798 cm/s, and the required flow rate of nitrogen was 37.59 LPM. The diameter of the reactor was determined to be 2.5 inch for 1.5, 2, 2.5, and 3-fold multiples of the minimum fluidization velocity.

- Calculation of minimum fluidization velocity (Ergun Eq.):

$$U_{mf}=\frac{\mu}{d_p\rho_g}\left\{\left[33.7^2+0.0408\frac{d_p^3\rho_g(\rho_s-\rho_g)g}{\mu^2}\right]^{\frac{1}{2}}-33.7\right\} \quad (1)$$

- Calculation of terminal velocity of coal particle (Re∈2-500):

$$U_t=1.53\left[\frac{gd^{1.6}\rho_g(\rho_s-\rho_g)}{\rho_g^{0.4}\mu^{0.6}}\right]^{0.714} \quad (2)$$

Table 3. Design process for bench-scale fluidized bed

Procedure	Decision item	Note
1	Capacity	1 kW (20 kg/day)
2	Reaction time	Residence time & kinetic data using lab-scale results
3	Volume	Bed material L_h/D
4	Diameter of reactor	Volume and U_{mf}
5	Distributor	Calculated by fluidization engineering [54]
6	Height of reactor	Reaction zone/Freeboard (similar to lab-scale reactor)
7	Cyclone	Efficiency 80%
8	Check	Cold-bed test

Table 4. Volume and weight of bed material according to diameter of reactor

	H (cm, L_h/D=3)	Volume (cm^3)	Weight (g)
	7.62	38.59	5.55
	11.43	130.24	180.74
ID	15.24	308.73	428.42
	19.05	602.99	836.77
	22.86	1041.97	1445.94

- Calculation of initial porosity in fluidized bed Archimedes constant:

$$Ar = \frac{gd^3\rho_g(\rho_s-\rho_g)}{\mu^2} \quad (3)$$

$$Re = \frac{du\rho}{\mu} \quad (4)$$

$$\varepsilon_0 = Ar^{-0.21}(18Re_{mf}+0.36Re_{mf}^2)^{0.21} \quad (5)$$

- Calculation of porosity in fluidized bed:

$$\varepsilon = \frac{u\varepsilon_0}{1.05u\varepsilon_0+(1-\varepsilon_0)U_{mf}} \quad (6)$$

- Calculation of expansion ratio in fluidized bed:

$$\frac{L_f}{L_{mf}} = \frac{1-\varepsilon_0}{1-\varepsilon} \quad (7)$$

Fifth, the diameter of the distributor was set at 0.5 Ø by considering the flow process and size of the coal particles; the number of holes was set at 48. *Fluidization Engineering* [39] was used as a reference in making this decision. Sixth, the height of the reactor was determined. The internal diameter of the reaction zone was 6.35 cm; the height of the reaction zone was 100 cm; the diameter of the free board was 12.7 cm; and the height of the free board was 87.5 cm; the similarities to the lab-scale reactor were considered when sizing the bench-scale fluidized bed catalytic gasification reactor. Seventh, a high efficiency standard-type cyclone was selected. The cyclone was selected by reference to Strauss (1975). Finally, fluidization in a cold-bed reactor was evaluated after performing a hot-test using the bench-scale fluidized bed.

RESULTS AND DISCUSSION

The catalytic-steam coal gasification experiment used lab- and bench-scale bubble fluidized bed reactors. The effect of varying the temperature on the gasification reaction characteristics was evaluated (600 °C, 700 °C, and 800 °C); the catalyst loading used herein was, respectively, 0 wt%, 5 wt%, and 10 wt% for physical mixing, and 10 wt% for impregnation, and the H_2O/C mole ratio was set to unity while using Indonesian lignite, MSJ, and Roto South coal samples in the lab-scale bubble fluidized bed reactor. The bench-scale bubble fluidized bed reaction was performed using the optimum conditions determined from the lab-scale results.

1. Effect of Operating Temperature in the Lab-scale Bubble Fluidized Bed

Steam gasification requires temperatures above 800 °C to proceed if no catalyst is added and is a highly endothermic reaction [3]. The use of a catalyst can significantly enhance the steam gasification reaction, and commercially acceptable gas production rates may be achieved at temperatures much lower than 800 °C [5,13]. Thus, catalytic-steam coal gasification was evaluated herein at temperature below 800 °C. In general, a low temperature leads to an increase in CH_4 production and decrease of CO and H_2. Although it is ideal to lower the gasification temperature in order to obtain highly concentrated CH_4, lower temperatures decrease the reactivity of coal towards gasification. Therefore, experiments were conducted under different temperature conditions in order to promote

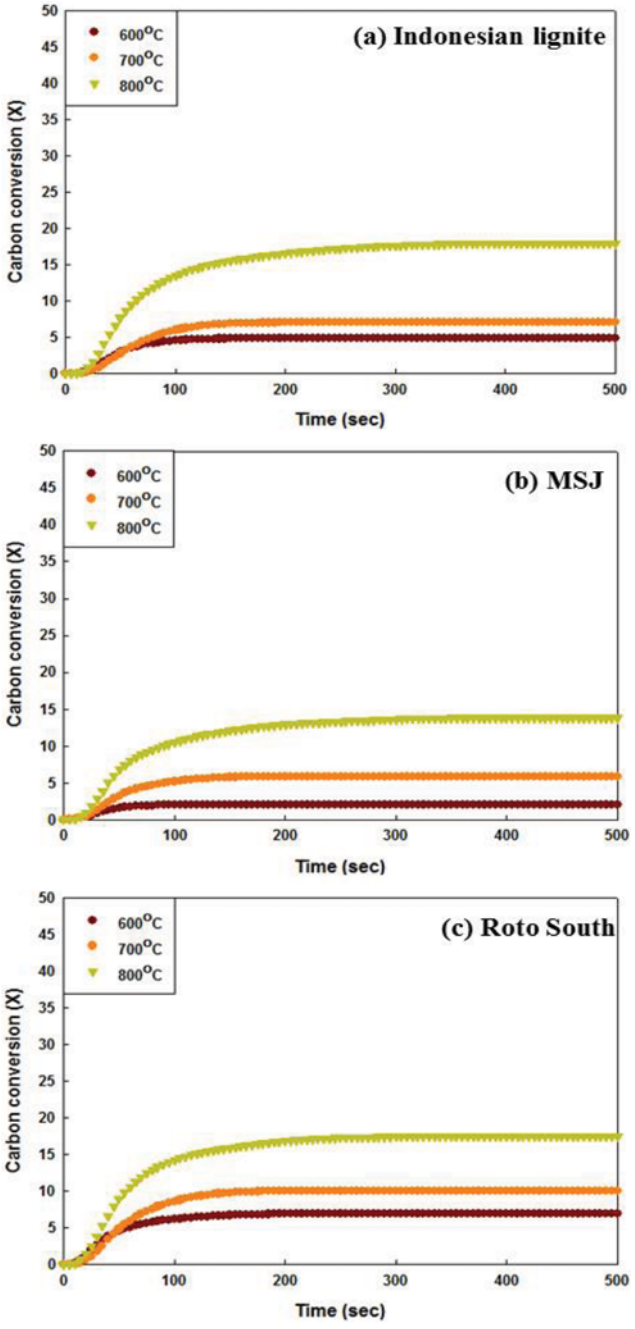

Fig. 3. Comparing of carbon conversion at different temperatures (H_2O/C mole ratio: 1, non-catalyst).

the gasification reaction [40]. The H_2O/C mole ratio was set to unity and the experiments were conducted at the respective temperatures (600 °C, 700 °C, and 800 °C) without the injection of a catalyst. The results of these experiments are shown in Fig. 3.

The results obtained at the respective temperatures indicated that none of the three coal samples produced H_2 at 600 °C. In addition, the generation of H_2, CO_2, CO, and CH_4 increased as the temperature increased, and the product yield (ml/s), indicated as the total volume/total reaction time, also increased over time. The syngas composition was greatly influenced by the temperature. In particular, the H_2 content was the most sensitive to temperature. Comparison of the syngas compositions achieved at the different temperatures confirmed that the mole ratios of H_2/CO, H_2/CO_2, CO/CO_2, and H_2/CH_4 increased as the temperature increased. This is because the production of H_2 increased as the temperature increased. The content of H_2 and CO increased with increasing temperature due to the steam-coal endothermic gasification reaction [41]. As mentioned in the literature [42], the production of hydrogen and carbon monoxide decreases at lower temperatures, and this tendency was confirmed in this study. The optimum reaction temperature was determined to be 800 °C based on consideration of the carbon conversion, cold gas efficiency, and syngas composition.

2. Effect of Catalyst (K_2CO_3) in the Lab-scale Bubble Fluidized Bed

To identify the effect of the catalyst injection method on the syngas composition, catalytic coal gasification was carried out at a fixed temperature of 800 °C, which was previously determined to be the optimum temperature for syngas production based on the results mentioned above. The data obtained using different catalyst injection protocols are summarized in Fig. 4. The amount of catalyst used in the experiment was varied, while the temperature was set to 800 °C and the H_2O/C mole ratio was fixed at unity.

Use of the catalyst resulted in increased syngas production for all the samples; the impregnation method had a greater influence on H_2 production than physical mixing. Increasing the K_2CO_3 loading led to an increase of the reaction rate. However, the results suggested a saturation point (indicated by a loss of reactivity due to increased catalyst injection), as an excess of the catalyst mixture accumulated in the pores of the coal particles, thereby reducing the contact surface of the porous carbon, which limited the coal gasification [37]. Furthermore, different results were obtained when the same catalyst was used for the different coals due to the characteristic differences between the coals. When impregnated coal was used in the cases of Indonesian lignite and MSJ, the H_2 produced exceeded 800 ml, whereas just over 700 ml of H_2 was produced with Roto South. The main effect of K_2CO_3 under atmospheric pressure was considered to be enhanced production of H_2. Hauserman (1994) and Timple et al. (1997) reported that the use of K_2CO_3 as a catalyst in steam gasification produced more hydrogen [43,44]. The catalytic-steam gasification production of H_2 increased when K_2CO_3 was used in the steam-coal reaction and was much higher than that achieved with non-catalytic gasification [41]. Many researchers have reported catalytic-steam gasification mechanisms for K_2CO_3 [19,45,46]. Despite such great efforts, a realistic gasification mechanism is not well-known. Some researchers suggested the following reaction mechanisms [19,45,47-50]:

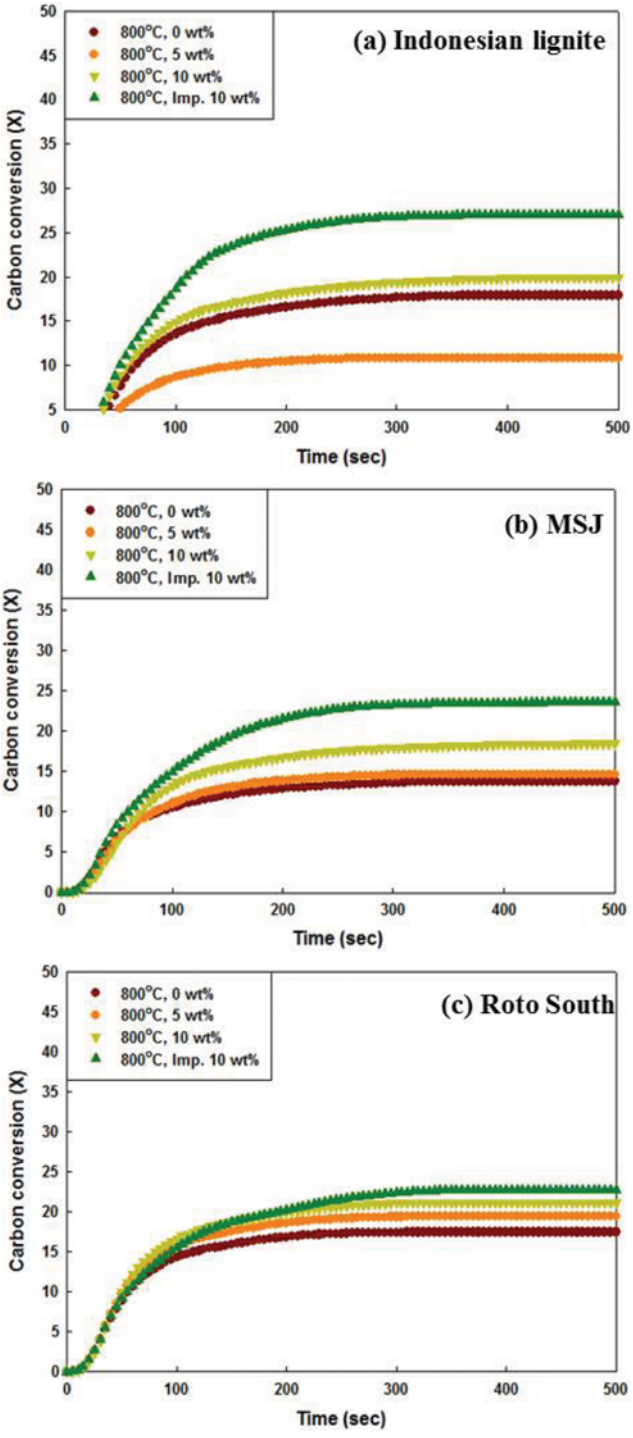

Fig. 4. Comparison of carbon conversion at 800 °C and H_2O/C mole ratio of unity with different catalyst loading.

$$K_2CO_3+2C \leftrightarrow 2K+3CO$$
$$2K+2_nC \leftrightarrow 2C_nK$$
$$2C_nK+2H_2O \leftrightarrow 2NC+2KOH+H_2$$
$$2KOH+CO \leftrightarrow K_2CO_3+H_2$$

Fig. 5 shows the compositions of the syngas products obtained

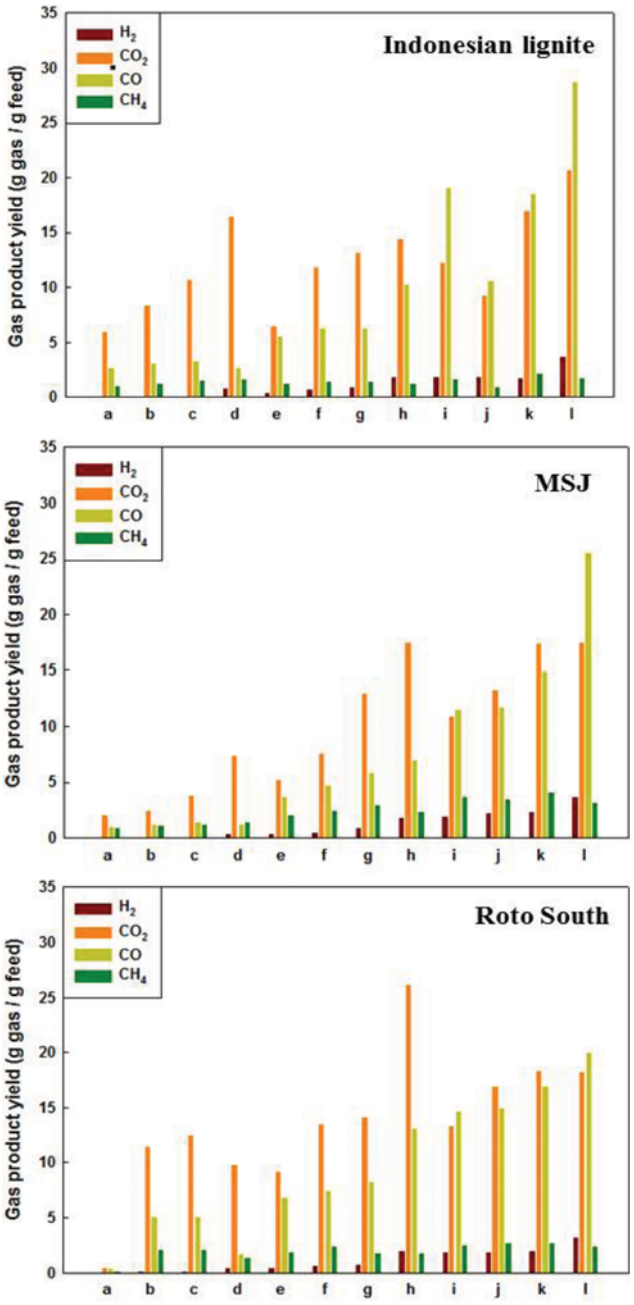

Fig. 5. Comparison effects of reaction temperature on gas product yield (g gas/g feed) for different catalysts in catalytic-steam gasification (a: catalyst 0 wt% at 600 °C, b: catalyst 5 wt% at 600 °C, c: catalyst 10 wt% at 600 °C, d: catalyst 10 wt% impregnation at 600 °C, e: catalyst 0 wt% at 700 °C, f: catalyst 5 wt% at 700 °C, g: catalyst 10 wt% at 700 °C, h: catalyst 10 wt% impregnation at 700 °C, i: catalyst 0 wt% at 800 °C, j: catalyst 5 wt% at 800 °C, k: catalyst 10 wt% at 800 °C, l: catalyst 10 wt% impregnation at 800 °C.

at different temperatures. Wang et al. (2009) reported that no H_2 production was observed at 600 °C in non-catalytic gasification, whereas catalytic gasification produced H_2 at 600 °C [51]. The same was found in this study. In addition, the H_2 production in this study was similar to that reported by Wang et al. (2009) for temperatures above 700 °C. The present results showed 'H_2 production per input coal (g gas/g feed)' values of 1.73 for Indonesian lignite, 1.76 for MSJ, and 1.92 for Roto South at 700 °C. Wang et al. (2009) reported 'H_2 production per input coal (g gas/g fed)' values of 1.8 at 700 °C and 2.1 at 750 °C for Chinese Huaibei bituminous coal, with 750 °C being the optimal temperature for hydrogen production.

In catalytic-steam gasification, the production of H_2 and CO increased to a greater extent than production of CO_2 and CH_4 with increasing temperature. This means that in commercial gasification, production of H_2 and CO is also expected to increase with increasing temperature. In commercial catalytic-steam gasification, the main sources of H_2 and CO production with increasing temperature can be summarized as follows [52]:

$C+H_2O \rightarrow CO+H_2$ (water gas reaction)

$Coal+Heat \rightarrow CO+H_2$ (coal pyrolysis reaction)

At higher temperatures, more CO is produced. This implies that at higher temperatures, CO production is driven by the Boudouard reaction [53]. This result corroborates the finding by Kumar et al. (2009) that at a higher temperature, the Boudouard reaction becomes predominant. Catalytic-steam gasification is driven predominantly by the water gas reaction, and at higher temperatures it is driven by the Boudouard reaction [54]. The extent of the increase of H_2 and CO production achieved using K_2CO_3 as a catalyst was larger at relatively high temperatures, similar to the results of other studies [55,56]. CH_4 production was minimally affected by the reaction temperature, and the amount of CH_4 produced from catalytic gasification/pyrolysis was found to be lower than that from non-catalytic gasification/pyrolysis. This may be due to the decomposition of CH_4 by the catalyst [56]. Tomita et al. (1985) reported that the H_2 content in the product gas was enhanced by the decomposition of CH_4, light hydrocarbon, and tar [17]. Dhirendra et al. (1986) evaluated the effect of K_2CO_3 on the gasification of high ash Indian coal at reaction temperatures of 500 °C-800 °C in a fluidized bed gasifier [57]. Furthermore, as previously mentioned, the production of syngas increased as a result of the effect of the catalyst, whereas the production of H_2 was enhanced with the use of the impregnation method instead of the physical mixing method. Evaluation of the carbon conversion, cold gas efficiency, and H_2 production indicated that impregnation with 10 wt% K_2CO_3 produced the optimal results.

3. Reaction Kinetics of Catalytic-steam Gasification in the Lab-scale Fluidized Bed

The derived results were applied to implementation of the gasification kinetic parameters. The gasification reaction is typically influenced by factors such as the inherent reaction of carbon within coal or char, the catalysis of inorganic materials, and the pore structure [58,59]. Therefore, the same sample can have different gasification rates due to the differences in reactivity, and various kinetic models have been proposed to account for these differences. In the coal reaction, homogeneous and heterogeneous reactions produce syngas as a major product of coal char, as shown in reactions (8)-(13) [60-63].

Oxidation: $C+O_2 \rightarrow CO_2/C+1/2O_2 \rightarrow CO$ (8)

Boudouard: $C+CO_2 \rightarrow 2CO$ (9)

Water gas: $C+H_2O \rightarrow CO+H_2 / C+2H_2O \rightarrow CO_2+2H_2$ (10)

Methanation: $C+2H_2 \rightarrow CH_4$ (11)

Water-gas shift: $CO+H_2O \rightarrow CO_2+H_2$ (12)

Steam reforming: $CH_4+H_2O \rightarrow CO+3H_2$ (13)

Gas-solid reaction models have been applied to quantitatively assess the gasification reaction kinetics and analyze the reactivity. A heterogeneous gas-solid reaction model was developed using the volumetric reaction model (VRM) [64] and shrinking core model (SCM) [65,66]. In this paper, the carbon conversion is expressed by Eq. (14).

$$\text{Carbon conversion} = \frac{\text{Quantity of carbon of syngas}}{\text{Input quantity of carbon}} \quad (14)$$

The input quantity of carbon is expressed using the amount of carbon determined by ultimate analysis and the input coal mass. The quantity of carbon in the syngas is expressed as the sum of the amount of carbon in carbon monoxide, carbon dioxide, and methane.

The VRM simplifies the coal-gas reaction, which is a heterogeneous reaction, into a homogeneous reaction, and assumes that

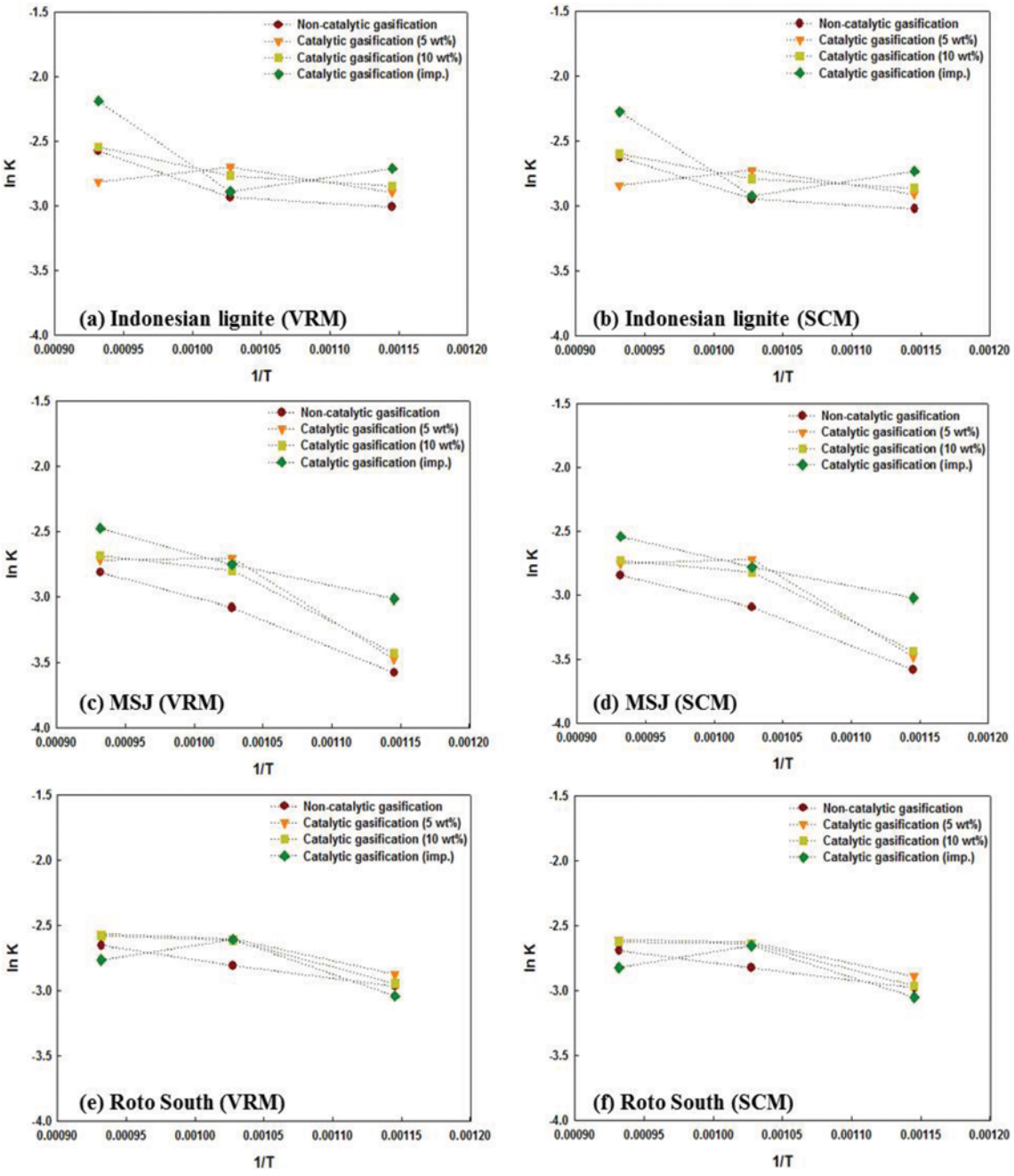

Fig. 6. Arrhenius plot (ln K vs. 1/T) for different catalyst loading using VRM and SCM.

Table 5. Values of E and A depanding on experimental parameters at H_2O/C mole ration of 1

Cat. (wt%)	Indonesian lignite		MSJ		Roto south	
	E (KJ/mol)	A (1/min)	E (KJ/mol)	A (1/min)	E (KJ/mol)	A (1/min)
VRM (Volumetric reaction model)						
0	16.50	0.45	30.01	1.78	12.17	0.27
5	3.56	0.09	30.29	2.24	12.35	0.31
10	11.56	0.27	29.56	2.03	14.65	0.41
Imp.	19.04	0.80	20.83	0.85	11.48	0.25
SCM (Shrinking core model)						
0	15.14	0.37	28.92	1.53	11.15	0.23
5	3.08	0.08	29.25	1.93	11.38	0.27
10	10.09	0.22	28.07	1.65	13.55	0.34
Imp.	16.67	0.56	18.65	0.63	9.65	0.19

the gas reacts uniformly wherever a reaction is possible both inside and outside the coal. The size of the coal is the same, and the density is reduced as the reaction progresses. This reaction is expressed by Eq. (15).

$$\frac{dx}{dt} = k(1-X), -\ln(1-X) \quad (15)$$

The SCM assumes that reaction of the gas starts at the surface of the char during the initial reactions; as the gas gradually enters the char, reaction is initiated at the unreacted core surface. Therefore, the size of the particle available for reaction is reduced, and the reaction is expressed by Eq. (16).

$$\frac{dx}{dt} = k(1-X)^{2/3},\ 3 = [1-(1-X)^{1/3}] = kt \quad (16)$$

Here, k in the above SCM and VRM equations indicates the rate constant, and relies on the Arrhenius equation, as expressed in Eq. (17)

$$k = A\exp\left(-\frac{E}{RT}\right) \quad (17)$$

A indicates the pre-exponential factor, E is the activation energy, R is the gas constant, and T is the absolute temperature. Fig. 6 shows Arrhenius plots for different experimental conditions using the VRM and SCM.

As shown in Fig. 6, the use of coal (not char) for non-catalytic gasification can generate reliable kinetic data, although the data fluctuated significantly with variation of the catalyst loading and input temperature during the catalytic gasification. This result can be explained in terms of the properties of K_2CO_3 in the catalytic gasification, as described below.

The catalytic effect decreases with increasing temperature, and catalysts are more effective in the gasification process if steam is present in the gasification gases. There is usually an optimum catalyst content beyond which either negligible or negative effects are observed. The relative effects of catalysts can differ under different reaction conditions. The gasification reactivity can be significantly affected by the method/condition of catalyst impregnation. Catalyst impregnation is more effective than physical mixing with carbon [33,45,67-70]. Furthermore, the catalytic-steam gasification reaction is slow below 750 °C. This implies that the catalyst activity is significantly influenced by the reaction temperature in catalytic gasification [51,71,72]. Furthermore, Freriks et al. (1981) reported that potassium formation from the catalyst is thermodynamically unfavorable below 827 °C, which implies that no catalytic effect can occur below 827 °C [73].

Table 5 shows the activation energies and pre-exponential factors obtained at different temperatures for fluidized bed catalytic gasification. The experimental data and the values applied in the model showed that when the H_2O/C mole ratio was unity, the activation energy of the impregnated coal was lower than that of the raw coal.

The activation energy of catalytic gasification was higher than that of non-catalytic gasification. Due to catalyst saturation, which induces a reactivity loss, accumulation of excess mixed catalyst in the pores of the coal reduces the surface area of coal, limiting the gasification reaction and resulting in a high activation energy [37]. Kuhn and Plogmann (1983) reported that excess K_2CO_3 caused a loss in the catalytic activity [12]. However, a lower catalyst loading can lead to reduced reaction due to the mineral matter in the coal, along with deactivation of the catalyst [55]. Wang et al. (2009) reported that a catalyst content of less than 7.5% was almost ineffective for catalytic gasification [51]. When using a single catalyst, the reaction rate may decline due to the rapid deactivation of the catalyst through poisoning and sintering, contact loss between the reactant and catalyst, catalyst volatilization, and catalyst encapsulation by carbon deposition.

From kinetic analysis of the catalytic-steam gasification, the lower activation energy obtained with the use of char showed that when the catalyst is added, only the reaction with carbon needs to be considered under the reaction conditions. On the other hand, the experiments with coal showed an increased activation energy [33]. Wang et al. (2009) reported that regardless of the catalyst loading and steam input, the catalytic-steam gasification reaction occurs at 750 °C, which means that kinetic analysis of the reaction with coal is more difficult than that with char [51]. In addition, efforts to record accurate kinetic data were hampered by the thermal decomposition reaction, followed by the gasification reaction

with coal. The experimental data and model data expressing the reaction kinetics of catalytic-steam gasification in one step were accurate only in the initial reaction and then showed large differences. It is believed that the use of a batch-type reactor instead of a continuous type reactor affected completion of the reaction, improvement in the reactivity due to increased temperature, and limitation of the mass transfer [74]. In other studies, when the same catalyst was used, the activation energy differed depending on the coal [39,66,75]. This means that the results obtained herein differ from those documented in the literature. Therefore, it was found that the H_2O/C mole ratio and catalyst feed method exerted significant effects on the reactivity with respect to the catalytic-steam gasification with steam. In summary, the input K_2CO_3 catalyst content and method and the use of steam in the coal catalytic-steam gasification process could increase the gasification efficiency [14].

4. Reaction of Bench-scale Catalytic Gasification Using Indonesian MSJ

For bench-scale catalytic-steam gasification, the Indonesian MSJ raw coal was impregnated with 10 wt% catalyst (K_2CO_3), the temperature was set at 800 °C, the H_2O/C mole ratio was unity, the gas velocity was fixed at 1.5 times the U_{mf}, the coal feeding rate was 17 g/min, and the side feeding method was employed under continuous operation for over 2 h after reaching steady state. Fig. 7 shows the data for the bench-scale fluidized bed catalytic-steam gasification reaction.

Empirical analysis of the bench-scale fluidized bed catalytic-steam gasification reaction indicated that the reaction could reach steady state within 30 min, and the hydrogen production volume was the highest. The catalytic-steam gasification experiments using the bench-scale fluidized bed reactor were conducted in the steady state. The results of continuous operation for 2 h after reaching steady state indicated that the total syngas production was as follows:

H_2: 931 L, CO_2: 401 L, CO: 190 L, CH_4: 49 L for raw coal; H_2: 2,434 L, CO_2: 1,148 L, CO: 336 L, and CH_4: 208 L for impregnated coal. Bench-scale catalytic-steam gasification at steady state produced a H_2/CO mole ratio of above 5 for syngas. This is higher than the H_2/CO mole ratio of non-catalytic gasification, which is approximately 4. These results show that the reactivity of impregnated coal was better than that of raw coal. From Fig. 7, the total content of H_2, CO_2, CO, and CH_4 in the production gases was also obtained for the non-catalytic and catalytic gasification. In the catalytic-steam gasification, the production of H_2 and CO_2 increased greatly compared to that in the non-catalytic gasification.

Fig. 8 shows the amount of synthesis gas produced at a given time. The accumulated amount of generated gas increased proportionally, while the amount of generated synthesis gas did not vary. Therefore, it is concluded that the experiment was conducted at the steady state using the bench-scale fluidized bed as shown in

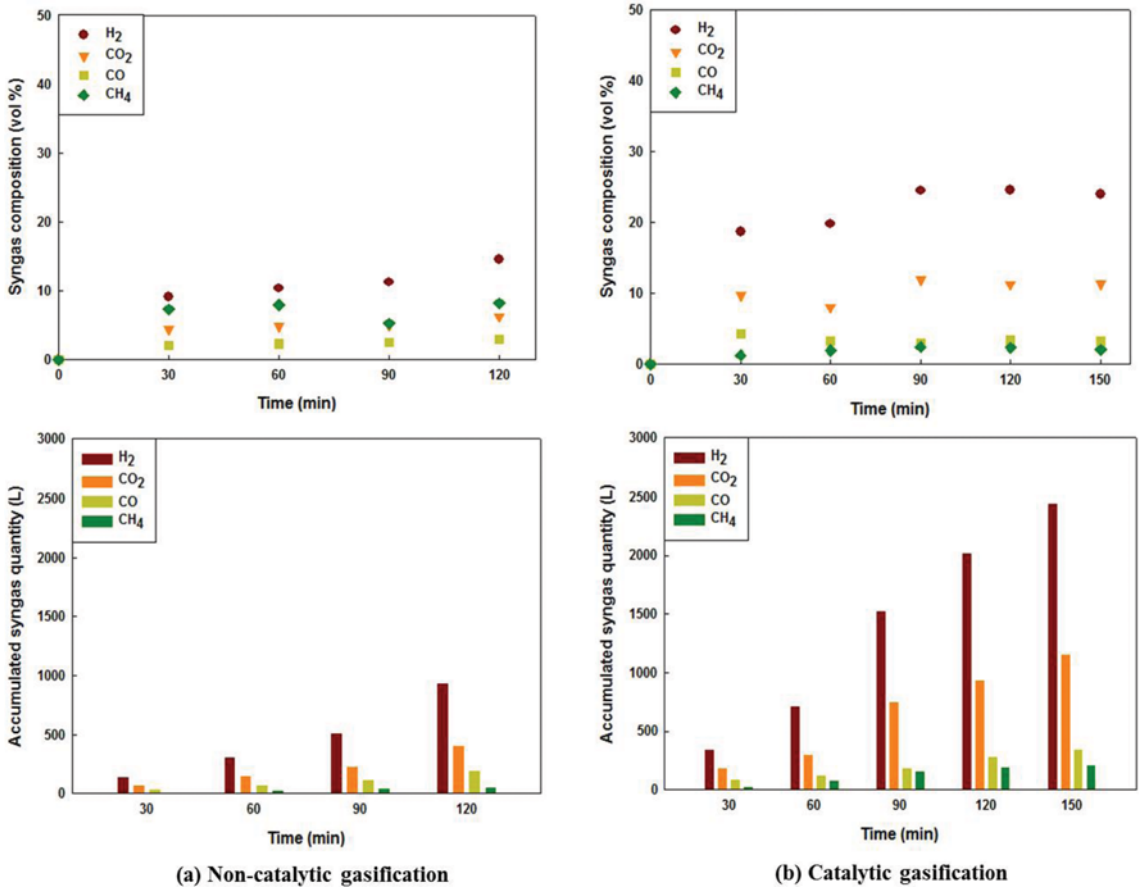

Fig. 7. Results of bench-scale catalytic-steam gasification using MSJ coal ((a) raw coal, (b) impregnated coal).

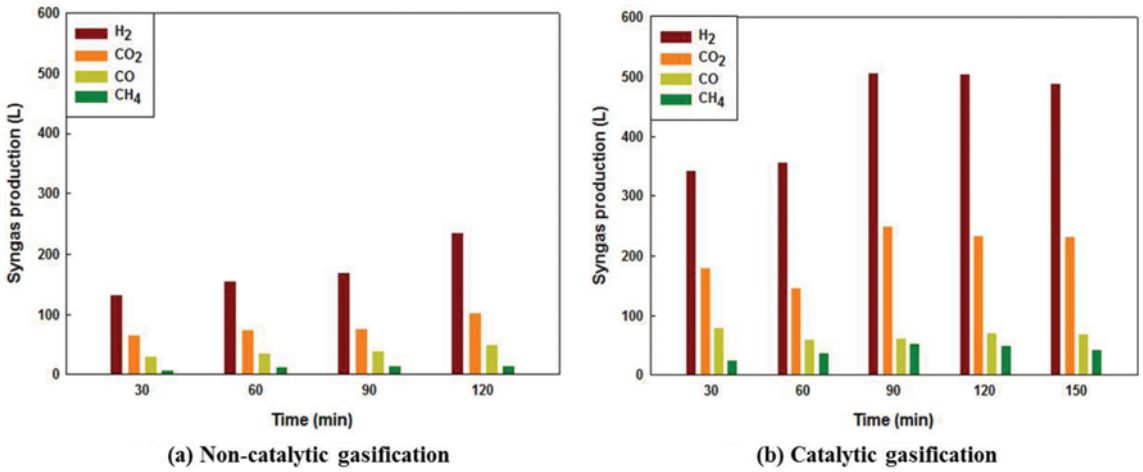

Fig. 8. Results of syngas production at estimated time using bench-scale catalytic-steam gasification with MSJ ((a) raw coal, (b) impregnated coal).

Fig. 7. Moreover, 200 L of H_2 was produced in the non-catalytic gasification, while the catalytic-steam gasification yielded 500 L of H_2. The carbon conversion of raw coal was approximately 30%, and the cold gas efficiency was approximately 31%. Compared to the decreased production of CO, CO_2, and H_2 in the non-catalytic gasification, the decrease in the production of CO_2 and H_2 was more remarkable for the catalytic-steam gasification, with substantially less formation of CO.

The catalytic-steam gasification of char can be expressed by the water gas and water gas shift reactions [51]. Based on the reaction mechanisms, catalytic-steam gasification not only leads to lower CO production but also to higher H_2 production. The rate of syngas formation increased in the catalytic-steam gasification. In addition, the results showed that catalytic-steam gasification did not greatly influence the CO/CO_2 ratio, in agreement with the results reported by Sharma et al. (2008) and Wang et al. (2009) [51,76]. In the case of impregnated coal, the carbon conversion and cold gas efficiency were approximately 63% based on the H_2, CO_2, CO, and CH_4 production data. Comparison of the results presented by Lee et al. (2001) with the current results showed that steady state was achieved faster in this study, with a higher carbon conversion and cold gas efficiency [56]. Lee et al. (2001) reported that the reactor required 40 min to attain steady state and the carbon version was 57% and the cold gas efficiency was 44% under the best conditions. In addition, Lee et al. (1998) reported that the carbon conversion for Australian sub-bituminous coal was the highest (45%) and the cold gas efficiency was the highest (35%) at 900 °C with the use of the impregnation technique employing 10 wt% of a mixed catalyst ($Ni(CO_3)_2+K_2SO_4$) [41].

A minimum heating value of more than 1,000 kcal/Nm^3 is possible in the operation of a gas engine [77]. The heating value with the supply of N_2 of the bench-scale catalytic gasification syngas operation is approximately 1,070 kcal/Nm^3 and without the supply of N_2 is approximately 2,560 kcal/Nm^3. Therefore, it is expected to facilitate the operation of a gas engine that functions primarily by producing syngas through the catalytic gasification of low rank coal. Catalytic-steam gasification with steam is a strongly endothermic process because of the water gas and water gas shift reaction [51]. In a commercial plant, the heating value and cold gas efficiency will be much lower than those of this study because the reaction will depend on the heating value of coal itself rather than external heating. In catalytic gasification, since gasification can occur at low temperatures of 700-750 °C, it is possible to supply the heat from an external heat source. However, in a commercial plant, air is generally used as an oxidant, which is energy consuming [13].

CONCLUSIONS

Low rank coals were subjected to lab-scale gasification and the efficiency of the gasification reaction was evaluated. The kinetic conditions and properties of the generated synthesis gas were demonstrated to be related to the reaction conditions. The residence time and kinetic data obtained using a lab-scale reactor was further applied to the design of a reactor for bench-scale fluidized bed catalytic gasification. The bench-scale reactor was successfully designed by considering the similarity of reactor volume and L_h/D to those of the lab-scale congener.

1) During catalytic-steam gasification, the activation energy varies based on the catalyst loading and temperature; the activation energy can appear high because of loss during the reaction, derived from saturation with the catalyst, where an excess of the mixed catalyst accumulates in the pores of the coal to decrease the surface area, thereby limiting the gasification reaction.

2) Based on analysis of the composition of syngas obtained by catalytic-steam gasification, the water gas reaction and water gas shift reaction were found to be the main reactions. Thus, syngas formation was significantly affected by the temperature and catalyst injection method.

3) Using the developed bench-scale fluidized bed catalytic-steam gasification system, high calorific syngas (1,070 kcal/Nm^3) was obtained; compared to that from a previous study, the time required to reach steady state was reduced by about 10 min, and the carbon conversion was improved by 20%.

4) The direct method of catalytic-steam gasification using low

rank coal produced the most H_2 at atmospheric pressure. It was also found that the catalytic gasification of low rank coal under experimental conditions of 800 °C, H_2O/C mole ratio of 1 and 10 wt% impregnated catalyst can be applied to coal to liquid (CTL).

ACKNOWLEDGEMENTS

This work was supported by the New & Renewable Energy of the Korea Institute of Energy Technology Evaluation and Planning (KETEP) grant funded by the Korea government Ministry of Trade, Industry & Energy (No. 20113020050010). This work was supported by the Korea Institute of Energy Technology Evaluation and Planning (KETEP) under Energy Efficiency and Resources Programs with Project number of 20132010201750.

NOMENCLATURE

U_{mf} : minimum fluidization velocity [cm/sec]
L_h : length [cm]
D : diameter [cm]
LPM : liters per minute
μ : viscosity [Pa·S]
dp : particle diameter of coal and sand particle [cm]
ρ_g : density of the gas [g/cm^3]
ρ_s : density of coal and sand [g/cm^3]
g : acceleration due to gravity [980 cm/s^2]
Re : Reynolds number
U_t : terminal velocity [cm/sec]
Ar : Archimedes number
ε, ε_{mf}, ε_0 : void fraction in the emulsion phase of a bubbling bed
L_f : height of a bubbling fluidized bed [cm]
L_{mf} : bed height at minimum fluidizing conditions [cm]
E : activation energy [kJ/mol]
A : pre-exponential factor [1/min]
R : gas constant [J/molK]
T : absolute temperature [K]
X : carbon conversion
t : time [min]
k : rate constant associated with temperature

REFERENCES

1. Intergovernmental Panel on Climate Change, Climate Change 2014: Mitigation of Climate Change (Vol. 3), Cambridge University Press (2015).
2. World Energy Resources: Coal World Energy Council (2013).
3. T. Takarada, Y. Tamai and A. Tomita, *Fuel*, **64**(10), 1438 (1985).
4. F. Huhn, J. Klein and H. Jüntgen, *Fuel*, **62**(2), 196 (1983).
5. N. C. Nahas, *Fuel*, **62**(2), 239 (1983).
6. T. Wigmans, R. Elfring and J. A. Moulijn, *Carbon*, **21**(1), 1 (1983).
7. D. W. McKee, C. L. Spiro, P. G. Kosky and E. J. Lamby, *Fuel*, **62**(2), 217 (1983).
8. K. J. Hüttinger and R. Minges, *Fuel*, **64**(4), 486 (1985).
9. R. J. Lang, *Fuel*, **65**(10), 1324 (1986).
10. T. Takarada, S. Ichinose and K. Kato, *Fuel*, **71**(8), 883 (1992).
11. H. Kubiak, H. J. Schröter, A. Sulimma and K. H. van Heek, *Fuel*, **62**(2), 242 (1983).
12. L. Kühn and H. Plogmann, *Fuel*, **62**(2), 205 (1983).
13. H. Jüntgen, *Fuel*, **62**(2), 234 (1983).
14. A. Triantoro and D. Diniyati, *J. Novel Carbon Resource Sciences*, **7**, 68 (2013).
15. S. J. Yuh and E. E. Wolf, *Fuel*, **62**(6), 738 (1983).
16. G. Bruno, M. Buroni, L. Carvani, G. Del Piero and G. Passoni, *Fuel*, **67**(1), 67 (1988).
17. A. Tomita, Y. Watanabe, T. Takarada, Y. Ohtsuka and Y. Tamai, *Fuel*, **64**(6), 795 (1985).
18. P. K. Bakkerud, *Catal. Today*, **106**(1), 30 (2005).
19. W. Y. Wen, Mechanisms of alkali metal catalysis in the gasification of coal, char, or graphite. *Catal. Rev.—Sci. Eng.*, **22**(1), 1 (1980).
20. X. Yuan, L. Zhao, H. Namkung, T. J. Kang and H. T. Kim, *Fuel Processing Technol.*, **141**, 44 (2016).
21. C. A. Euker and R. A. Reitz, Exxon catalytic coal gasification process development program. *Final Project Report for the U. S. Department of Energy under Contract No. ET-78-C-01-2777* (1981).
22. A. C. Sheth, C. Sastry, Y. D. Yeboah, Y. Xu and P. Agarwal, *J. Air Waste Manage. Association*, **53**(4), 451 (2003).
23. X. Yuan, *Performance evaluation of potassium catalyst recovery process in the K_2CO_3-catalyzed steam gasification system*, Ajou University (2016).
24. S. H. Lee and S. D. Kim, *Korean Chem. Eng. Res.*, **46**(3), 443 (2008).
25. J. M. Lee, Y. J. Kim, W. J. Lee and S. D. Kim, *Hwahak Konghak*, **35**(1), 121 (1997).
26. D. W. McKee, *Carbon*, **20**(1), 59 (1982).
27. Z. L. Liu and H. H. Zhu, *Fuel*, **65**(10), 1334 (1986).
28. A. Karimi and M. R. Gray, *Fuel*, **90**(1), 120 (2011).
29. T. Suzuki, M. Mishima, J. Kitaguchi, M. Itoh and Y. Watanabe, *Fuel Processing Technol.*, **8**(3), 205 (1984).
30. C. L. Spiro, D. W. Mckee, P. G. Kosky and E. J. Lamby, *Fuel*, **62**(2), 180 (1983).
31. P. J. Walker Jr., M. Shelef and R. A. Anderson, Catalysis of carbon gasification, *Chem. Phys. Carbon; (United States)*, 4 (1968).
32. D. A. Sams, T. Talverdian and F. Shadman, *Fuel*, **64**(9), 1208 (1985).
33. E. J. Hippo and D. Tandon, *Preprints of Papers-american Chemical Society Division Fuel Chemistry*, **41**, 216 (1996).
34. F. J. Long and K. W. Sykes, *J. Chim. Phys.*, **47**, 361 (1950).
35. D. W. McKee, *Carbon*, **12**(4), 453 (1974).
36. W. L. Holstein and M. Boudart, *Fuel*, **62**(2), 162 (1983).
37. Y. T. Kim, D. K. Seo and J. H. Hwang, *Korean Chem. Eng. Res.*, **49**(3), 372 (2011).
38. T. J. Kang, H. Namkung, L. H. Xu, H. Park, K. Hakizimana, J. De Dieu and H. T. Kim, *Asia-Pacific J. Chem. Eng.*, **11**(2), 237 (2016).
39. D. Kunii and O. Levenspiel, *Fluidization Engineering*, Elsevier (2013).
40. J. Y. Park, D. K. Lee, S. C. Hwang, S. K. Kim, S. H. Lee, S. K. Yoon, J. H. Yoo, S. H. Lee and Y. W. Rhee, *Clean Technol.*, **19**(3), 306 (2013).
41. J. M. Lee, Y. J. Kim and S. D. Kim, *Appl. Therm. Eng.*, **18**(11), 1013 (1998).
42. Y. Liu, J. Qian and J. Wang, *Fuel Processing Technol.*, **63**(1), 45 (2000).
43. W. B. Hauserman, *Int. J. Hydrogen Energy*, **19**(5), 413 (1994).
44. R. C. Timpe, R. W. Kulas, W. B. Hauserman, R. K. Sharma, E. S.

Olson and W. G. Willson, *Int. J. Hydrogen Energy*, **22**(5), 487 (1997).
45. D. W. McKee, *Fuel*, **62**(2), 170 (1983).
46. J. M. Saber, J. L. Falconer and L. F. Brown, *J. Catal.*, **90**(1), 65 (1984).
47. B. J. Wood and K. M. Sancier, *Catal. Rev. Sci. Eng.*, **26**(2), 233 (1984).
48. J. Wang, K. Sakanishi, I. Saito, T. Takarada and K. Morishita, *Energy Fuels*, **19**(5), 2114 (2005).
49. M. Matsukata, T. Fujikawa, E. Kikuchi and Y. Morita, *Energy Fuels*, **2**(6), 750 (1988).
50. J. Kopyscinski, M. Rahman, R. Gupta, C. A. Mims and J. M. Hill, *Fuel*, **117**, 1181 (2014).
51. J. Wang, M. Jiang, Y. Yao, Y. Zhang and J. Cao, *Fuel*, **88**(9), 1572 (2009).
52. O. C. Kural, (Ed.), *Coal: resources, properties, utilization, pollution*, Istanbul Technical University (1994).
53. D. Tristantini, D. Supramono and R. K. Suwignjo, *Int. J. Technol.*, **6**, 22 (2015).
54. A. Kumar, D. D. Jones and M. A. Hanna, *Energies*, **2**(3), 556 (2009).
55. W. J. Lee and S. D. Kim, *Fuel*, **74**(9), 1387 (1995).
56. W. J. Lee, S. D. Kim and B. H. Song, *Korean J. Chem. Eng.*, **18**(5), 640 (2001).
57. M. Vajpeyi, S. K. Awasthi and G. N. Pandey, *Energy*, **11**(6), 563 (1986).
58. K. Miura, K. Hashimoto and P. L. Silveston, *Fuel*, **68**(11), 1461 (1989).
59. S. Kasaoka, Y. Sakata and C. Tong, *Int. Chem. Eng.; (United States)*, **25**(1) (1985).
60. F. Bustamante, R. M. Enick, A. V. Cugini, R. P. Killmeyer, B. H. Howard, K. S. Rothenberger, M. V. Ciocco, B. D. Morreale, S. Chattopadhyay and S. Shi, *AIChE J.*, **50**(5), 1028 (2004).
61. D. H. Lee, H. Yang, R. Yan and D. T. Liang, *Fuel*, **86**(3), 410 (2007).
62. H. Thunman, F. Niklasson, F. Johnsson and B. Leckner, *Energy Fuels*, **15**(6), 1488 (2001).
63. F. Yan, S. Y. Luo, Z. Q. Hu, B. Xiao and G. Cheng, *Bioresour. Technol.*, **101**(14), 5633 (2010).
64. M. Ishida and C. Y. Wen, *AIChE J.*, **14**(2), 311 (1968).
65. C. Y. Wen, *Ind. Eng. Chem.*, **60**(9), 34 (1968).
66. B. H. Song, Y. W. Jang and Y. S. Byeon, *Korean Chem. Eng. Res.*, **41**(3), 19 (2003).
67. D. A. Fox and A. H. White, *Ind. Eng. Chem.*, **23**(3), 259 (1931).
68. D. W. McKee and D. Chatterji, *Carbon*, **13**(5), 381 (1975).
69. D. A. Sams, T. Talverdian and F. Shadman, *Fuel*, **64**(9), 1208 (1985).
70. T. Wigmans, H. Haringa and J. A. Moulijn, *Fuel*, **62**(2), 185 (1983).
71. J. Wang, K. Sakanishi, I. Saito, T. Takarada and K. Morishita, *Energy Fuels*, **19**(5), 2114 (2005).
72. J. Wang, Y. Yao, J. Cao and M. Jiang, *Fuel*, **89**(2), 310 (2010).
73. I. L. Freriks, H. M. van Wechem, J. C. Stuiver and R. Bouwman, *Fuel*, **60**(6), 463 (1981).
74. Q. Liu, H. Hu, Q. Zhou, S. Zhu and G. Chen, *Fuel*, **83**(6), 713 (2004).
75. S. J. Seo, S. J. Lee and J. M. Sohn, *Clean Technol.*, **20**(1), 72 (2014).
76. A. Sharma, T. Takanohashi and I. Saito, *Fuel*, **87**(12), 2686 (2008).
77. C. Lee, S. M. Cho, Y. D. Yoo and Y. Yun, *Korea Soc. Energy Eng.*, 143 (2005).